Fair Spatial Indexing: A paradigm for Group Spatial Fairness

Sina Shaham
Viterbi School of Engineering
University of Southern California
Los Angeles, California, USA
sshaham@usc.edu

Gabriel Ghinita
College of Science and Engineering
Hamad Bin Khalifa University
Qatar Foundation, Doha, Qatar
gghinita@hbku.edu.qa

Cyrus Shahabi
Viterbi School of Engineering
University of Southern California
Los Angeles, California, USA
shahabi@usc.edu

ABSTRACT

Machine learning (ML) is playing an increasing role in decision-making tasks that directly affect individuals, e.g., loan approvals, or job applicant screening. Significant concerns arise that, without special provisions, individuals from under-privileged backgrounds may not get equitable access to services and opportunities. Existing research studies *fairness* with respect to protected attributes such as gender, race or income, but the impact of location data on fairness has been largely overlooked. With the widespread adoption of mobile apps, geospatial attributes are increasingly used in ML, and their potential to introduce unfair bias is significant, given their high correlation with protected attributes. We propose techniques to mitigate location bias in machine learning. Specifically, we consider the issue of miscalibration when dealing with geospatial attributes. We focus on *spatial group fairness* and we propose a spatial indexing algorithm that accounts for fairness. Our KD-tree inspired approach significantly improves fairness while maintaining high learning accuracy, as shown by extensive experimental results on real data.

1 INTRODUCTION

Recent advances in machine learning (ML) led to its adoption in numerous decision-making tasks that directly affect individuals, such as loan evaluation or job application screening. Several studies [4, 25, 27] pointed out that ML techniques may introduce bias with respect to protected attributes such as race, gender, age or income. The last years witnessed the introduction of *fairness* models and techniques that aim to ensure all individuals are treated equitably, focusing especially on conventional protected attributes (like race or gender). However, the impact of geospatial attributes on fairness has not been extensively studied, even though location information is being increasingly used in decision-making for novel tasks, such as recommendations, advertising or ride-sharing. Conventional applications may also often rely on location data, e.g., allocation of local government resources, or crime prediction by law enforcement using geographical features. For example, the Chicago Police Department releases monthly crime datasets [2] and classifies neighborhoods based on their crime risk level. Subsequently, the risk level is used to determine vehicle and house insurance premiums, which are increased to reflect the risk level, and in turn, result in additional financial hardship for individuals from under-privileged groups.

Fairness for geospatial data is a challenging problem, due to two main factors: (i) data are more complex than conventional protected attributes such as gender or race, which are categorical and have only a few possible values; and (ii) the correlation between locations and protected attributes may be difficult to capture accurately, thus leading to hard-to-detect biases.

We consider the case of *group fairness* [8], which ensures no significant difference in outcomes occurs across distinct population groups. In our setting, groups are defined with respect to geospatial regions. The data domain is partitioned into disjoint regions, and each of them represents a group. All individuals whose locations belong to a certain region are assigned to the corresponding group. In practice, a spatial group can correspond to a zip code, a neighborhood, or a set of city blocks. Our objective is to devise fair geospatial partitioning algorithms, which can handle the needs of applications that require different levels of granularity in terms of location reporting. *Spatial indexing* [9, 37, 40] is a common approach used for partitioning, and numerous techniques have been proposed that partition the data domain according to varying criteria, such as area, perimeter, data point count, etc. We build upon existing spatial indexing techniques, and adapt the partition criteria to account for the specific goals of fairness. By carefully combining geospatial and fairness criteria in the partitioning strategies, one can obtain spatial fairness while still preserving the useful spatial properties of indexing structures (e.g., fine-level clustering of the data).

Specifically, we consider a set of partitioning criteria that combines physical proximity and *calibration error*. Calibration is an essential concept in classification tasks which quantifies the quality of a classifier. Consider a binary classification task, such as a loan approval process. Calibration measures the difference between the observed and predicted probabilities of any given point being labeled in the positive class. If one partitions the data according to some protected attribute, then the expectation would be that the probability should be the same across both groups (e.g., people from different neighborhoods should have an equal chance, on aggregate, to be approved for a loan). If the expected and actual probabilities are different, that represents a good indication of unfair treatment.

Our proposed approach builds a hierarchical spatial index structure by using a composite split metric, consisting of both geospatial criteria (e.g., compact area) and miscalibration error. In doing so, it allows ML applications to benefit from granular geospatial information, while at the same time ensuring that no significant bias is present in the learning process.

Our specific contributions include:

- We identify and formulate the problem of spatial group fairness, an important concept which ensures that geospatial information can be used reliably in a classification task, without introducing, intentionally or not, biases against individuals from underprivileged groups;
- We propose a new metric to quantify unfairness with respect to geospatial boundaries, called Expected Neighborhood Calibration Error (ENCE);
- We propose a technique for fair spatial indexing that builds on KD-trees and considers both geospatial and fairness criteria, by lowering miscalibration and reducing ENCE;

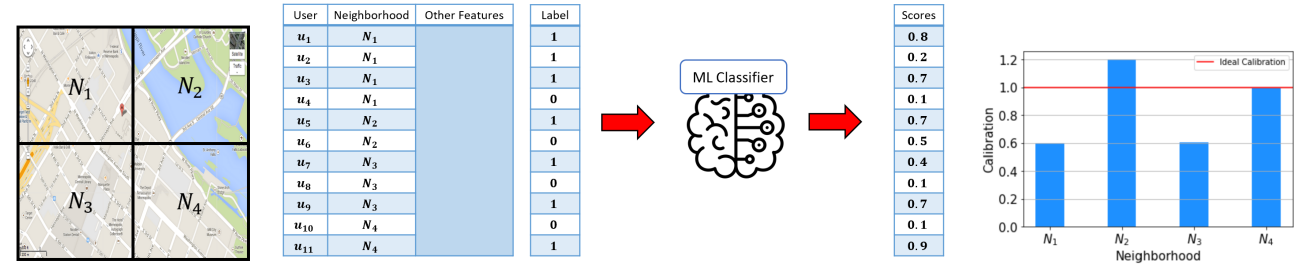

(a) Neighborhoods Partitioning (b) Generation of Classifier Scores (c) Calibration of Neighborhoods

Figure 1: An example of the miscalibration problem with respect to neighborhoods.

- We perform an extensive experimental evaluation on real datasets, showing that the proposed approach is effective in enforcing spatial group fairness while maintaining data utility for classification tasks.

The rest of the paper is organized as follows: Section 2 provides background and fundamental definitions. Section 3 reviews related work. We introduce the proposed fair index construction technique in Section 4. Section 5 presents the results of our empirical evaluation, followed by conclusions in Section 6.

2 BACKGROUND

2.1 System Architecture

We consider a binary classification task T over a dataset D of individuals $u_1, ..., u_{|D|}$. The feature set recorded for u_i is denoted by $\boldsymbol{x_i} \in \mathbb{R}^l$, and its corresponding label by $y_i \in \{0, 1\}$. Each record consists of l features, including an attribute called *neighborhood*, which captures an individual's location, and is the main focus of our approach. The sets of all input data and labels are denoted by $\mathcal{X}$ and $\mathcal{Y}$, respectively. A classifier $h(.)$ is trained over the input data resulting in $h(\mathcal{X}) = (\hat{Y}, \hat{S})$ where $\hat{\mathcal{Y}} = \{\hat{y}_1, ..., \hat{y}_{|D|}\}$ is the set of predicted labels ($\hat{y}_i \in \{0, 1\}$) and $\mathcal{S} = \{s_1, ..., s_{|D|}\}$ is the set of confidence scores ($s_i \in [0, 1]$) for each label.

The dataset's neighborhood feature indicates the individual's *spatial group*. We assume the spatial data domain is split into a set of partitions of arbitrary granularity. Without loss of generality, we consider a $U \times V$ grid overlaid on the map. The grid is selected such that its resolution captures adequate spatial accuracy as required by application needs. A set of neighborhoods is a non-overlapping partitioning of the map that covers the entire space, with the i^{th} neighborhood denoted by N_i, and the set of neighborhoods denoted by $\mathcal{N}$.

Figure 1 illustrates the system overview. Figure 1a shows the map divided into 4 non-overlapping partitions $\mathcal{N} = \{N_1, N_2, N_3, N_4\}$. The neighborhood is recorded for each individual $u_1, ..., u_{11}$ together with other features, and a classifier is trained over the data. The classifier's output is the confidence score for each entry which turns into a class label by setting a threshold.

2.2 Fairness Metric

Our primary focus is to achieve *spatial group fairness* using as metric the concept of *calibration* [26, 29], described in the following.

In classification tasks, it is desirable to have scores indicating the probability that a test data record belongs to a certain class. Probability scores are especially important in ranking problems, where top candidates are selected based on relative quantitative performance. Unfortunately, it is not granted that confidence scores generated by a classifier can be interpreted as probabilities. Consider a binary classifier that indicates an individual's chance of committing a crime after their release from jail (recidivism). If two individuals u_1 and u_2 get confidence scores 0.4 and 0.8, this cannot be directly interpreted as the likelihood of committing a crime by u_2 being twice as high as for u_1. The model *calibration* aims to alleviate precisely this shortcoming.

Definition 1. (Calibration). An ML model is said to be calibrated if it produces calibrated confidence scores. Formally, outcome score R is *calibrated* if for all scores r in support of R it holds that

$$P(y = 1|R = r) = r \tag{1}$$

This condition means that the set of all instances assigned a score value r contains an r fraction of positive instances. The metric is a group-level metric. Suppose there exist 10 people who have been assigned a confidence score of 0.7. In a well-calibrated model, we expect to have 7 individuals with positive labels among them. Thus, the probability of the whole group is 0.7 to be positive, but it does not indicate that every individual in the group has this exact chance of receiving a positive label.

To measure the amount of miscalibration for the whole model or for an output interval, the ratio of two key factors needs to be calculated: expected confidence scores and the expected value of true labels. Abiding by the convention in [26], we use functions $o(.)$ and $e(.)$ to return the true fraction of positive instances and the expected value of confidence scores, respectively. For example, the calibration of the model in Figure 1b is computed as:

$$\frac{e(h)}{o(h)} = \frac{(\sum_{u \in D} s_u)/|D|}{(\sum_{u \in D} y_u)/|D|} = \frac{5.2/11}{7/11} \approx .742 \tag{2}$$

Perfect calibration is achieved when a specific ratio is equal to one. Ratios that are above or below one are considered miscalibration cases. Another way to measure the calibration error is by using the absolute value of the difference between two values, denoted by $|e(h) - o(h)|$, with the ideal value being zero. In this work, the second method is utilized, as it eliminates the division by zero problem that may arise from neighborhoods with low populations.

2.3 Problem Formulation

Even when a model is overall well-calibrated, it can still lead to unfair treatment of individuals from different neighborhoods. In order to achieve spatial group fairness, we must have a well-calibrated model with respect to *all* neighborhoods. The existence of calibration error in a neighborhood can result in classifier bias and lead to systematic unfairness against individuals from that

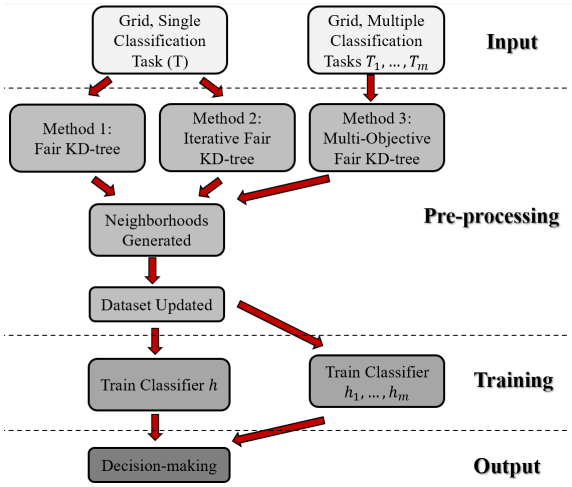

Figure 2: Overview of the proposed mitigation techniques.

neighborhood (in Section 5, we support this claim with real data measurements).

Definition 2. (Calibration for Neighborhoods). Given neighborhood set $\mathcal{N} = \{N_1, ..., N_t\}$, we say that the score R is calibrated in neighborhood N_i if for all the scores r in support of R it holds that

$$P(y = 1|R = r, N = N_i) = r, \qquad \forall i \in [1, t] \tag{3}$$

The following equations can be used to measure the amount of miscalibration with respect to neighborhood N_i,

$$\frac{e(h|N = N_i)}{o(h|N = N_i)} \quad \text{or} \quad |e(h|N = N_i) - o(h|N = N_i)| \tag{4}$$

Going back to the example in Figure 1d, the calibration amount for neighborhoods N_1 to N_4 is visualized on a plot. Neighborhood N_4 is well-calibrated, whereas the others suffer from miscalibration.

Problem 1. *Given* m *binary classification tasks* $T_1, T_2, ..., T_m$, *we seek to partition the space into continuous non-overlapping neighborhoods such that for each decision-making task, the trained model is well-calibrated for all neighborhoods.*

2.4 Evaluation Metrics

A commonly used metric to evaluate the calibration of a model is Expected Calibration Error (ECE) [13]. The goal of ECE (detailed in Appendix A.1) is to understand the validity of output confidence scores. However, our focus is on identifying the calibration error imposed on different neighborhoods. Therefore, we extend ECE and propose the Expected Neighborhood Calibration Error (ENCE) that captures the calibration performance over all neighborhoods.

Definition 3. (Expected Neighborhood Calibration Error). Given t non-overlapping geospatial regions $\mathcal{N} = \{N_1, ..., N_t\}$ and a classifier h trained over data located in these neighborhoods, the ENCE metric is calculated as:

$$\text{ENCE} = \sum_{i=1}^{t} \frac{|N_i|}{|D|} |o(N_i) - e(N_i)| \tag{5}$$

Table 1: Summary of Notations.

Symbol	Description
k	Number of features
$D = \{u_1, ..., u_{\|D\|}\}$	Dataset of individuals
(x_i, y_i)	(Set of features, true label) for u_i
$D = [\mathcal{X}, \mathcal{Y}]$	Dataset with user features and labels
$\hat{\mathcal{Y}}$=$\{\hat{y}_1, .., \hat{y}_{\|D\|}\}$	Set of predicted labels
$\mathcal{S} = \{s_1, ..., s_{\|D\|}\}$	Set of confidence scores
$\mathcal{N} = \{N_1, ..., N_t\}$	Set of neighborhoods
$U \times V$	Base grid resolution
T	Binary classification task
m	Number of binary classification tasks
t	Number of neighborhoods
t_h	Tree height

where $o(N_i)$ and $e(N_i)$ return the true fraction of positive instances and the expected value of confidence scores for instances in N_i[1].

3 RELATED WORK

Fairness in ML. There exist two broad categories of fairness notions [5, 24]: individual fairness and group fairness. In group fairness, individuals are divided into groups according to a protected attribute, and a decision is said to be fair if it leads to a desired statistical measure across groups. Some prominent group fairness metrics are calibration [29], statistical parity [21][7], equalized odds [14], treatment equality [4], and test fairness [6]. Individual fairness notions focus on treating similar individuals the same way. Similarity may be defined with respect to a particular task [7, 17].

Unfairness mitigation techniques can be categorized into three broad groups: pre-processing, in-processing, and post-processing. Pre-processing algorithms achieve fairness by focusing on the classifier's input data. Some well-known techniques include suppression of sensitive attributes, change of labels, reweighting, representation learning, and sampling [18]. In-processing techniques achieve fairness during training by adding new terms to the loss function [19] or including more constraints in the optimization. Post-processing techniques sacrifice the utility of output confidence scores and align them with the fairness objective [28].

Fairness in Spatial Domain. The fairness and justice concepts in geographical social studies have been a subject of research as early as the 1990's [15]. With the rise of ML and its influence on decision-making with geospatial data, this issue has gained increased importance. Neighborhoods or individual locations frequently serve as decision-making factors in entities such as government agencies and banks. This context can lead to unfairness in a variety of tasks, such as mortgage lending [22], job recruitment [10], school admissions [3], and crime risk prediction [36].

A case study on American Census datasets by Ghodsi et al. [12] underlines the context's importance for fairness, illustrating how spatial distribution can impact a model's fairness-related performance. According to [36], recidivism prediction models built with data from one location often underperform when applied

[1]Symbol |.| denotes absolute value.

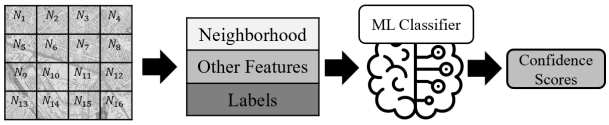

(a) Initial execution of classifier.

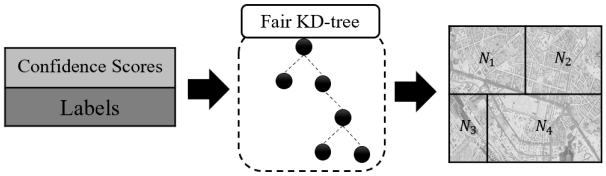

(b) Re-districting the map based on fairness objective.

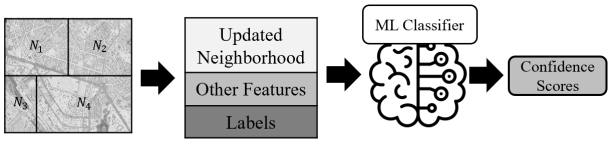

(c) Training classifier based on re-districted neighborhoods.

Figure 3: Overview of Fair KD-tree algorithm.

to another location. The study in [33] explores individual spatial fairness within two contexts: (i) distance-based fairness, motivated by nearest neighbor semantics, such as selecting drivers in ride-sharing apps, and (ii) zone-based fairness, where abrupt changes in neighborhood boundaries can bias the classifier's outcome. The work in [34] formulates the issue of fairness-aware range queries, defining a fair query as one most similar to the user's own query. Studies in [16, 39] consider crop monitoring in palm oil plantations, aiming to incorporate a fairness criterion primarily based on the $F1$ score during training. Additionally, the authors propose SPAD (space as a distribution) - a method to formulate the spatial fairness of learning models in continuous domains. The authors in [32] define spatial fairness as the statistical independence of outcomes from locations and propose an approach to audit spatial fairness. The auditing is conducted by exploring the distribution of outcomes inside and outside of a given region and how similar they are. Weydemann et al. [38] measure fairness in next-location recommendation systems in which the historical movement pattern of users is utilized to make future location recommendations. The proposed framework by the authors first captures the probability that the location recommender suggests locations based on race groups and then aims to adjust the distribution for fairer outcomes.

The authors in [31] propose a loss function designed for individual fairness in social media and location-based advertising. Pujol et al. [30] expose the disparate impact of differential privacy on various neighborhoods. There have been numerous attempts to apply fairness notions to clustering data points in Cartesian space. The notion described in[20] views clustering as fair if the average distance to points in its own cluster is not larger than the average distance to any other cluster's points. The authors in [23] concentrate on defining individual fairness for k-median and k-means algorithms, suggesting clustering is individually fair if each point expects to have a cluster center within a certain radius.

4 SPATIAL FAIRNESS THROUGH INDEXING

We introduce several algorithms that achieve group spatial fairness by constructing spatial index structures in a way that takes into account fairness considerations when performing data domain splits. We choose KD-trees as a starting point for our solutions, due to their ability to adapt to data density, and their property of covering the entire data domain (as opposed to structures like R-trees that may leave gaps within the domain).

Figure 2 provides an overview of the proposed solution. Our input consists of a *base grid* with an arbitrarily-fine granularity overlaid on the map, the attributes/features of individuals in the data, and their classification labels. The attribute set includes individual location, represented as the grid cell enclosing the individual. We propose a suite of three alternative algorithms for fairness, which are applied in the pre-processing phase of the ML pipeline and lead to the generation of new neighborhood boundaries. Once spatial partitioning is completed, the location attribute of each individual is updated, and classification is performed again.

The proposed algorithms are:

- *Fair KD-tree* is our primary algorithm and it re-districts spatial neighborhoods based on an initial classification of data over a base grid. Fair KD-tree can be applied to a single classification task.
- *Iterative Fair KD-tree* improves upon Fair KD-tree by refining the initial ML scores at every height of the index structure. It incurs higher computational complexity but provides improved fairness.
- *Multi-Objective Fair KD-tree* enables Fair KD-trees for multiple classification tasks. It leads to the generation of neighborhoods that fairly represent spatial groups for multiple objectives.

Next, we prove an important result that applies to all proposed algorithms, which states that any non-overlapping partitioning of the location domain has a weighted average calibration greater or equal to the overall model calibration. The proofs of all theorems are provided in Appendix A.

Theorem 1. *For a given model h and a complete non-overlapping partitioning of the space $\mathcal{N} = \{N_1, N_2, ..., N_t\}$, ENCE is lower-bounded by the overall calibration of the model.*

A broader statement can also be proven, showing that further partitioning leads to poorer ENCE performance.

Theorem 2. *Consider a binary classifier h and two complete non-overlapping partitioning of the space $\mathcal{N}_1$ and $\mathcal{N}_2$. If $\mathcal{N}_2$ is a sub-partitioning of $\mathcal{N}_1$, then:*

$$ENCE(N_1) \leq ENCE(N_2) \tag{6}$$

Neighborhood set $\mathcal{N}_2$ is a sub-partitioning of $\mathcal{N}_1$ if for every $N_i \in \mathcal{N}_1$, there exists a set of neighborhoods in $\mathcal{N}_2$ such that their union is N_i.

4.1 Fair KD-tree

We build a KD-tree index that partitions the space into non-overlapping regions according to a split metric that takes into account the miscalibration metric within the regions resulting after each split. Figure 3 illustrates this approach, which consists of three steps. Algorithm 1 presents the pseudocode of the approach.

Step 1. The base grid is used as input, where the location of each individual is represented by the identifier of their enclosing

Algorithm 1 Fair KD-tree

Input: Grid ($U \times V$), Features ($\mathcal{X}$), Labels ($\mathcal{Y}$), Height (t_h).
Output: New neighborhoods and updated feature set

1: **function** FairKDTree($N, \mathcal{X}, \mathcal{Y}, \mathcal{S}, t_h$)
2: **if** $t_h = 0$ **then**
3: $\mathcal{N} \leftarrow \mathcal{N} + N$
4: **return** $True$
5: $axis \leftarrow t_h$ **mod** 2
6: $L_{k^*}, R_{k^*} \leftarrow$ SplitNeighborhood($N, \mathcal{Y}, \mathcal{S}, axis$)
7: Run FairKDtree($L_{k^*}, \mathcal{X}, \mathcal{Y}, \mathcal{S}, t_h - 1$)
8: Run FairKDtree($R_{k^*}, \mathcal{X}, \mathcal{Y}, \mathcal{S}, t_h - 1$)
9: $N_1 \leftarrow$ Grid
10: **Global** $\mathcal{N} \leftarrow \{\}$
11: Set all neighborhoods in $\mathcal{X}$ to N_1
12: Scores ($\mathcal{S}$) $\leftarrow$ Train ML model on $\mathcal{X}$ and $\mathcal{Y}$
13: Neighborhoods ($\mathcal{N}$) $\leftarrow$ Run $FairKDtree(N_1, \mathcal{X}, \mathcal{Y}, \mathcal{S}, t_h)$
14: Update neighborhoods in $\mathcal{X}$
15: **return** $\mathcal{N}$, $\mathcal{X}$

Algorithm 2 Split Neighborhood

Input: Neighborhood (N), Confidence Scores ($\mathcal{S}$), Labels ($\mathcal{Y}$), Axis.
Output: Non-overlapping split of N into two neighborhoods

1: **function** SplitNeighborhood($N, \mathcal{S}, \mathcal{Y}, axis$)
2: **if** $axis = 1$ **then**
3: $N \leftarrow$ Transpose of N
4: $U' \times V' \leftarrow$ Dimensions of N
5: **for** $k = 1...U'$ **do**
6: $L_k \leftarrow$ Neighborhoods in $1...k$
7: $R_k \leftarrow$ Neighborhoods in $k+1...U$
8: $z_i \leftarrow$ Compute Equation (9) for L_k and R_k
9: $k^* \leftarrow \arg\min_k \; z_k$
10: **return** L_{k^*}, R_{k^*}

grid cell. This location attribute, alongside other features, is used as input to an ML classifier h for training. The classifier's output is a set of confidence scores $\mathcal{S}$, as illustrated in Figure 3a. Once confidence scores are generated, the true fraction of positive instances and the expected value of predicted confidence scores of the model with respect to neighborhoods can be calculated as follows:

$$e(h|N = N_i) = \frac{1}{|N_i|}\Big(\sum_{u \in N_i} s_u\Big) \qquad \forall i \in [1, t] \tag{7}$$

$$o(h|N = N_i) = \frac{1}{|N_i|}\Big(\sum_{u \in N_i} y_u\Big) \qquad \forall i \in [1, t] \tag{8}$$

where t is the number of neighborhoods.

Step 2. This step performs the actual partitioning, by customizing the KD-tree split algorithm with a novel objective function. KD-trees are binary trees where a region is split into two parts, typically according to the median value of the coordinate across one of the dimensions (latitude or longitude). Instead, we select the division index that reduces the fairness metric, i.e., ENCE miscalibration. Confidence scores and labels resulted from the previous training step are used as input for the split point decision. For a given tree node, assume the corresponding partition covers $U' \times V'$ cells of the entire $U \times V$ grid. Without loss of generality, we consider partitioning on the horizontal axis (i.e., row-wise). The aim is to find an index k which groups rows 1 to k into one node and rows $k+1$ to U' into another, such that the fairness objective is minimized (among all possible index split positions). Let L_k and R_k denote the left and right regions generated by splitting on index k. The fairness objective for index k is:

$$z_k = \Big|\, |L_k| \times |o(L_k) - e(L_k)| - |R_k| \times |o(R_k) - e(R_k)\,| \Big| \tag{9}$$

In the above equation, $|L_k|$ and $|R_k|$ return the number of data entries in the left and right regions, respectively. The intuition behind the objective function is to reduce the model miscalibration difference as we heuristically move forward. Two key points about the above function are: (i) the formulation of calibration is used in linear format due to the possibility of a zero denominator, and (ii) the calibration values are weighted by their corresponding regions' cardinalities. The optimal index k^* is selected as:

$$k^* = \arg\min_k \; z_k \tag{10}$$

Step 3. On completion of the fair KD-tree algorithm, the index leaf set provides a non-overlapping partitioning of the map. In the algorithm's final step, the neighborhood of each individual in the dataset is updated according to the leaf set and used for training.

The pseudocode for the Fair KD-tree method is illustrated in Algorithms 1 and 2. The *SplitNeighborhood* function in the latter identifies the split point based on the fairness goal, and it is invoked multiple times within Algorithm 1. In Algorithm 1, lines 9 to 12 outline the algorithm's initial training stage, as detailed previously in Step 1. The starting grid is determined as N_1 in line 9, and the model undergoes training in line 12. The recursive split procedure is initiated in line 13. Upon reaching a leaf node, the neighborhood is stored in line 3. If not, further divisions are made, focusing on the fairness target.

Theorem 3. *For a given dataset D, the required number of neighborhoods t and the model h, the computational complexity of Fair KD-tree is $O(|D| \times \lceil \log(t) \rceil) + O(h)$.*

4.2 Iterative Fair KD-tree

One drawback of the Fair KD-tree algorithm is its sensitivity to the initial execution of the model, which uses the baseline grid to generate confidence scores. Even though the space is recursively partitioned following the initial steps, the scores are not re-computed until the index construction is finalized. The

Algorithm 3 Iterative Fair KD-tree

Input: Grid ($U \times V$), Features ($\mathcal{X}$), Labels ($\mathcal{Y}$), Height (t_h).
Output: New neighborhoods and updated feature set

1: $N_1 \leftarrow$ Grid
2: Set all neighborhoods in $\mathcal{X}$ to N_1
3: $\mathcal{N} \leftarrow \{N_1\}$
4: **while** $t_h > 0$ **do**
5: Scores ($\mathcal{S}$) $\leftarrow$ Train ML model on $\mathcal{X}$ and $\mathcal{Y}$
6: $\mathcal{N}_{\text{new}} \leftarrow \{\}$
7: **for** N_i in $\mathcal{N}$ **do**
8: $L, R \leftarrow$ SplitNeighborhood($N_i, \mathcal{S}, \mathcal{Y}, t_h\%2$)
9: $\mathcal{N}_{\text{new}} \leftarrow \mathcal{N}_{\text{new}} + L, R$
10:
$\mathcal{N} \leftarrow \mathcal{N}_{\text{new}}$
11: Update neighborhoods in $\mathcal{X}$ based on $\mathcal{N}$
12: $t_h \leftarrow t_h - 1$
13: **return** $\mathcal{N}$, $\mathcal{X}$

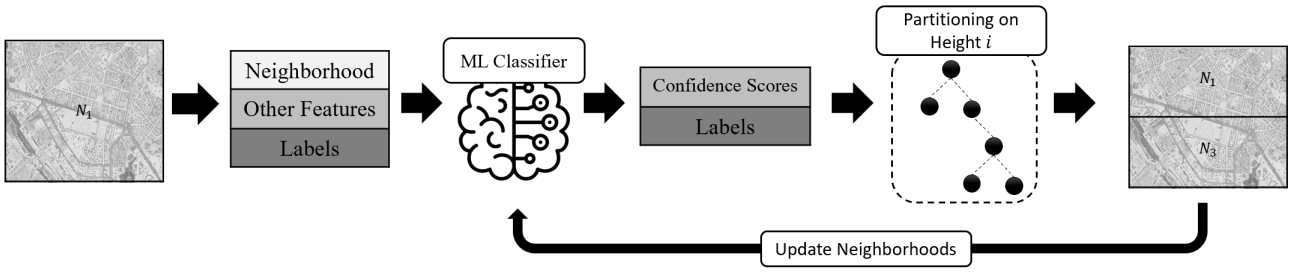

Figure 4: Overview of Iterative Fair KD-tree algorithm.

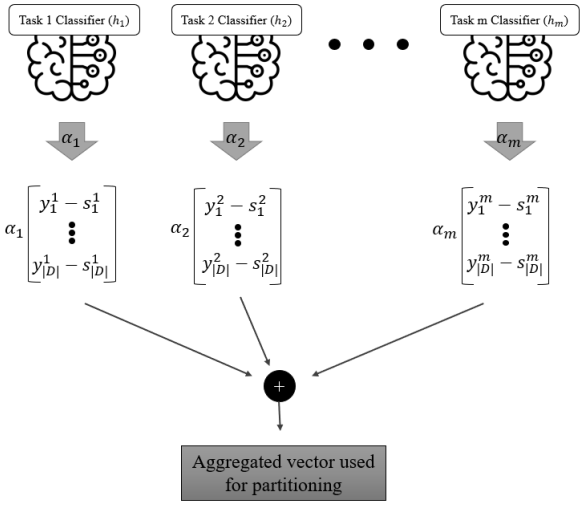

Figure 5: Aggregation in Multi-Objective Fair KD-tree.

iterative fair KD-tree addresses this limitation by re-training the model and computing updated confidence scores after each split (i.e., at each level of the tree). A refined version of ML scores is used at every height of the tree, leading to a more fair redistricting of the map.

Similar to the Fair KD-tree algorithm, the baseline grid is initially used, and all grid cells are considered to be in the same neighborhood (i.e., a single spatial group covering the entire domain). The algorithm is implemented in t_h iterations with the root node corresponding to the initial point (entire domain). As opposed to the Fair KD-tree algorithm that follows Depth First Search (DFS) recursion, the Iterative Fair KD-tree algorithm is based on Breadth First Search (BFS) traversal. Therefore, all nodes in the given height $i-1$ are completed before moving forward to the height i. Suppose we are in the i^{th} level of the tree, and all nodes at that level are generated. Note that, the set of nodes at the same height represents a non-overlapping partitioning of the grid. The algorithm continues by updating the neighborhoods at height i based on the $i-1$ level partitioning. Then, the updated dataset is used to train a new model, thus updating confidence scores for each individual.

Algorithm 3 presents the Iterative Fair KD-tree algorithm. Let $\mathcal{N}$ denote the set of all neighborhoods at level i of the tree. For each neighborhood $N_i \in \mathcal{N}$, Iterative Fair KD-tree splits the region N_i by calling the *SplitNeighborhood* function in Algorithm 2. The split is done on the x-axis if i is even and on the y-axis otherwise.

The algorithm provides a more effective way of determining a fair neighborhood partitioning by re-training the model at every tree level, but incurs higher computation complexity.

Theorem 4. *For a given dataset D, the required number of neighborhoods t and the model h, the computational complexity of Iterative Fair KD-tree is $O(|D| \times \lceil \log(t) \rceil) + \lceil \log(t) \rceil \times O(h)$.*

4.3 Multi-Objective Fair KD-tree

So far, we focused on achieving a fair representation of space given a *single* classification task. In practice, applications may dictate multiple classification objectives. For example, a set of neighborhoods that are fairly represented in a city budget allocation task may not necessarily result in a fair representation of a map for deriving car insurance premia. Next, we show how Fair KD-tree can be extended to incorporate multi-objective decision-making tasks.

We devise an alternative method to compute initial scores in Line 8 of Algorithm 2, which can then be called as part of Fair KD-tree in Algorithm 1. A separate classifier is trained over each task to incorporate all classification objectives. Let h_i be the i^{th} classifier trained over D and label set $\mathcal{Y}_i$ representing the task T_i. The output of the classifier is denoted by $\mathcal{S}_i = \{s_1^i, ..., s_{|D|}^i\}$, where in s_j^i, the superscript identifies the set $\mathcal{S}_i$ and the subscript indicates individual u_j. Once confidence scores for all models are generated, an auxiliary vector is constructed as follows:

$$\boldsymbol{v}_i = \begin{bmatrix} s_1^i - y_1^i \\ s_2^i - y_2^i \\ \vdots \\ s_{|D|}^i - y_{|D|}^i \end{bmatrix}, \qquad \forall i \in [1...t] \tag{11}$$

To facilitate task prioritization, hyper-parameters $\alpha_1, ..., \alpha_m$ are introduced such that $\sum_{i=1}^m \alpha_i = 1$ and $0 \leq \alpha_i \leq 1$. Coefficient α_i indicates the significance of classification T_i. The complete vector used for computing the partitioning is then calculated as,

$$\boldsymbol{v}_{tot} = \sum_{i=1}^{m} \alpha_i \boldsymbol{v}_i = \begin{bmatrix} \sum_{i=1}^m \alpha_i (s_1^i - y_1^i) \\ \sum_{i=1}^m \alpha_i (s_2^i - y_2^i) \\ \vdots \\ \sum_{i=1}^m \alpha_i (s_{|D|}^i - y_{|D|}^i) \end{bmatrix} \tag{12}$$

In the above formulation, each row corresponds to a unique individual and captures its role in all classification tasks. Let $\boldsymbol{v}_{tot}[u_i]$ denote the entry corresponding to u_i in $\boldsymbol{v}_{tot}$. Then the classification objective function in Eq. 9 is replaced by:

$$z_k = \Big| \, |L_k| \times | \sum_{u_i = L_k} \boldsymbol{v}_{tot}[u_i]| \; - \; |R_k| \times | \sum_{u_i = R_k} \boldsymbol{v}_{tot}[u_i] \, | \Big| \tag{13}$$

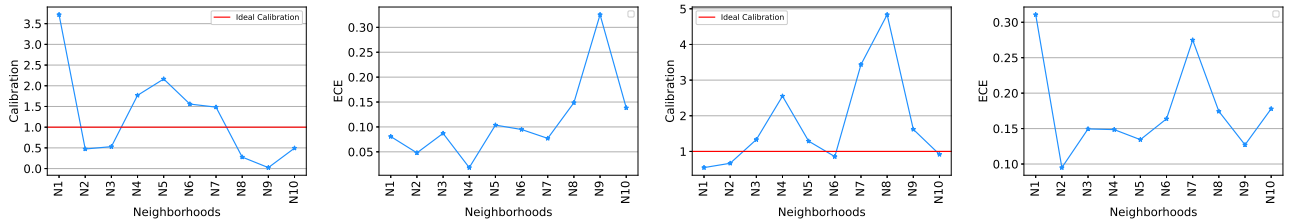

(a) EdGap (Los Angeles) (b) EdGap (Los Angeles) (c) EdGap (Houston) (d) EdGap (Houston)

Figure 6: Evidence of Model Disparity on Geospatial Neighborhoods.

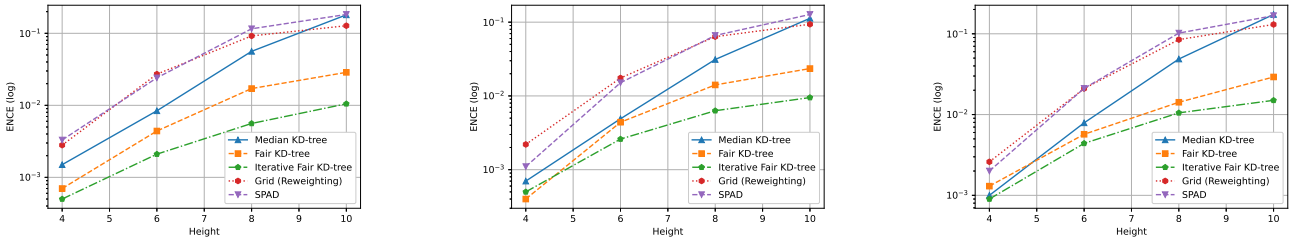

(a) Los Angeles (Logistic Regression) (b) Los Angeles (Decision Tree) (c) Los Angeles (Naive Bayes)

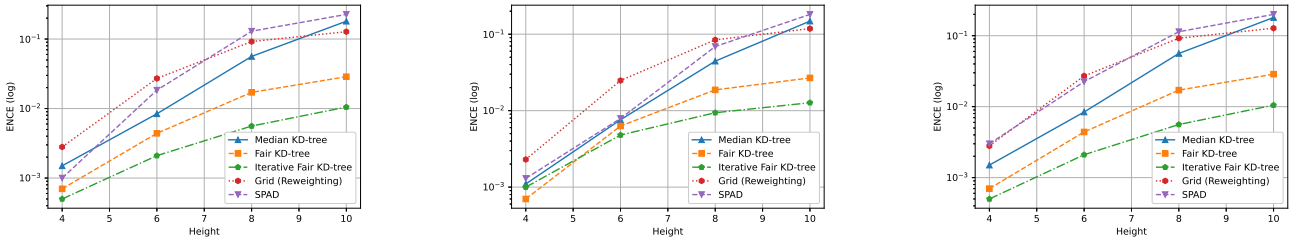

(d) Houston (Logistic Regression) (e) Houston (Decision Tree) (f) Houston (Naive Bayes)

Figure 7: Performance Evaluation with respect to ENCE.

and the optimal split point is selected as,

$$k^* = \arg\min_k \quad z_k \tag{14}$$

Vector aggregation is illustrated in Figure 5.

Theorem 5. *For a given dataset D, the required number of neighborhoods t and m classification tasks modelled by $h_1, ..., h_m$, computational complexity of Multi-Objective Fair KD-tree is $O(|D| \times \lceil \log(t) \rceil) + \sum_{i=1}^{m} O(h_i)$.*

5 EXPERIMENTAL EVALUATION

5.1 Experimental Setup

We use two real-world datasets provided by EdGap [35] with 1153 and 966 data records respectively, containing socio-economic features (e.g., household income and family structure) of US high school students in Los Angeles, CA and Houston, Texas. Consistent with [11], we use two features of average American College Testing (ACT) and the percentage of family employment as indicators to generate classification labels. The geospatial coordinates of schools are derived by linking their identification number to data provided by the National Center for Education Statistics [1].

We evaluate the performance of our proposed approaches (Fair KD-tree, Iterative Fair KD-tree, and multi-objective Fair KD-tree) in comparison with four benchmarks: (i) Median KD-tree, the standard method for KD-tree partitioning; (ii) Reweighting over grid – an adaptation of the re-weighting approach used in in [18] and deployed in geospatial tools such as *IBM AI Fairness 360*; (iii) Zipcode partitioning; and (iv) the SPAD (space as a distribution) method proposed in [39], designed to improve spatial fairness by minimizing statistical discrepancies tied to partitioning and scaling in a continuous space. The core idea of SPAD is to introduce fairness via a referee at the start of each training epoch. This involves adjusting the learning rate for different data sample partitions. Intuitively, a partition that exceeds performance expectations will receive a reduced learning rate, while those underperforming will be allocated higher rates. All experiments are implemented in Python and executed on a 3.40GHz core-i7 Intel processor with 16GB RAM.

5.2 Evidence for Disparity in Geospatial ML

First, we perform a set of experiments to measure the amount of bias that occurs when performing ML on geospatial datasets without any mitigating factors. Figure 6 captures the existing disparity with respect to widely accepted metrics of calibration error and ECE with 15 bins. We use the ratio representation of calibration in which a closer value to 1 represents higher calibration levels. Two logistic regression models are trained over neighborhoods in Los Angeles and Houston areas. The labels

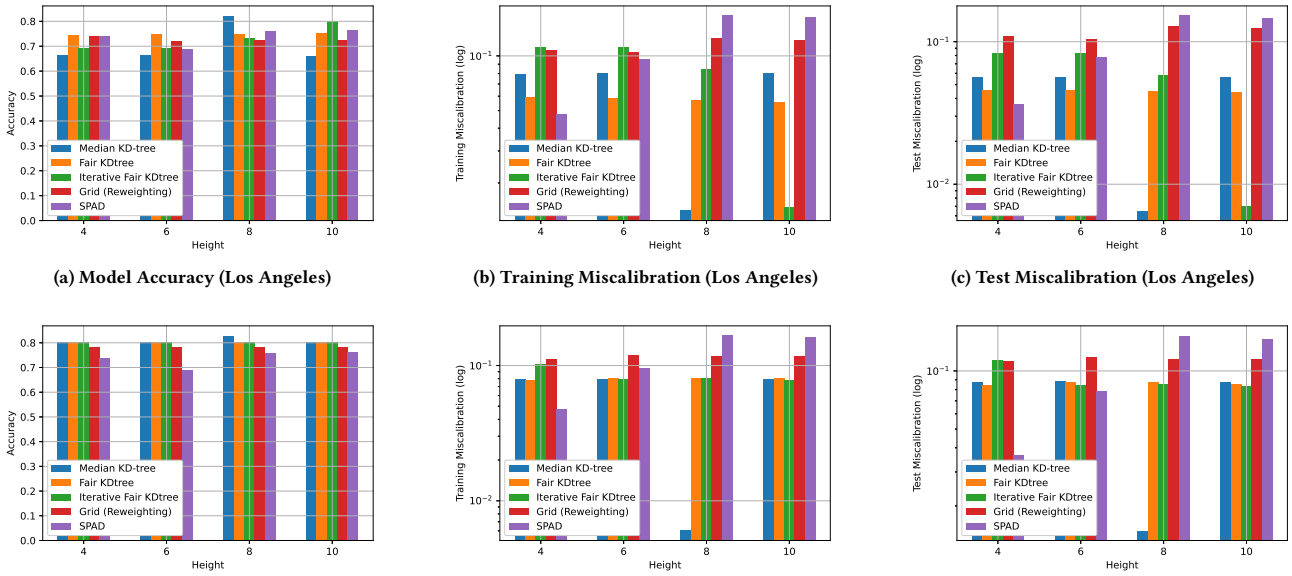

(a) Model Accuracy (Los Angeles)

(b) Training Miscalibration (Los Angeles)

(c) Test Miscalibration (Los Angeles)

(d) Model Accuracy (Houston)

(e) Training Miscalibration (Houston)

(f) Test Miscalibration (Houston)

Figure 8: Performance Evaluation with respect to other indicators.

are generated by setting a threshold of 22 on the average ACT performance of students in schools. The overall performance of models in terms of training and test calibration in Los Angeles and Texas are $(1.005,\ 1.033)$ and $(0.999,\ 0.958)$, respectively. Both training and test calibration are close to 1 overall, which in a naive interpretation would indicate all schools are treated fairly. However, this is not the case when computing the same metrics on a per-neighborhood basis. Figure 6 shows miscaibration error for the top 10 most populated zip codes. Despite the model's acceptable outcomes *overall*, many *individual* neighborhoods suffer from severe calibration errors, leading to unfair outcomes in the most populated regions, which are often home to the under-privileged communities.

5.3 Mitigation Algorithms

5.3.1 Evaluation w.r.t. ENCE Metric. ENCE is our primary evaluation metric that captures the amount of calibration error over neighborhoods. Recall that Fair KD-tree and its extension Iterative Fair KD-tree can work for any given classification ML model. We apply algorithms for Logistic Regression, Decision Tree, and Naive Bayes classifiers to ensure diversity in models. We focus on student SAT performance following the prior work in [11] by setting the threshold to 22 for label generation. Figure 7 provides the results in Los Angeles and Houston on the EdGap dataset. The x-axis denotes the tree's height used in the algorithm. Having a higher height indicates a finer-grained partitioning. The y-axis is log-scale.

Figure 7 demonstrates that both Fair KD-tree and Iterative Fair KD-tree outperform benchmarks by a significant margin. The improvement percentage increases as the number of neighborhoods increase, which is an advantage of our techniques, since finer spatial granularity is beneficial for most analysis tasks. The intuition behind this trend lies in the overall calibration of the model: given that the trained model is well-calibrated overall, dividing the space into a smaller number of neighborhoods is expected to achieve a calibration error closer to the overall model. This result supports Theorem 1, stating that ENCE is lower-bounded by the number of neighborhoods. Iterative Fair KD-tree behaves better, as confidence scores are updated on every tree level. The improvement achieved compared to Fair KD-trees comes at the expense of higher computational complexity. On average Fair KD-tree achieves 45% better performance in terms of computational complexity. The time taken for Fair KD-tree with 10 levels is 102 seconds, versus 189 seconds for the iterative version.

5.3.2 Evaluation w.r.t. other Indicators. In Figure 8 we evaluate fairness with respect to three other key indicators: model accuracy, training miscalibration, and test miscalibration. We focus on logistic regression to discuss the performance as one of the most widely adopted classification units. The accuracy of all algorithms follows a similar pattern and increases at higher tree heights. This is expected, as more geospatial information can be extracted at finer granularities.

Figure 8b shows training miscalibration calculated for the overall model (a lower value of calibration error indicates better performance). Our proposed algorithms have comparable calibration errors to benchmarks, even though their fairness is far superior. Out of all benchmarks, SPAD is observed to have comparable or slightly better performance than our approach, but *only at coarse granularities*, when the space is partitioned according to a low-height structure. However, at coarse granularity, there is little information that is provided to the data recipient (e.g., in practice, it is of interest to take decisions at a city block granularity, whereas zipcode-scale granularity is too coarse). For finer-grained partitioning (i.e., higher height values) Fair KD-tree and iterative KD-tree outperform benchmarks.

To understand better the underlying performance trends, Figure 9 provides the heatmap for the tree-based algorithms over 10 different tree heights. The amount of contribution each feature has on decision-masking is captured using a different color code. One observation is that the model shifts focus to different features based on the height. Such sudden changes can impact the generated confidence scores and, subsequently, the overall

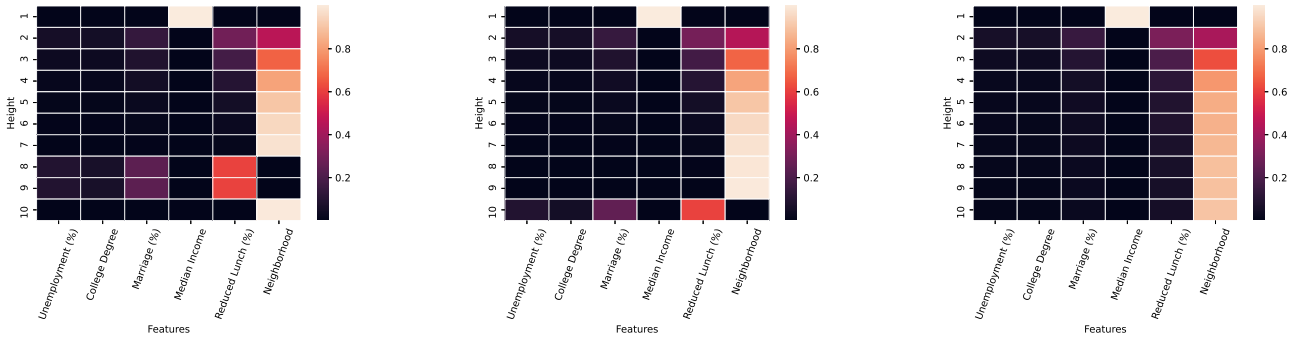

(a) Median KD-tree (Los Angeles) (b) Fair KD-tree (Los Angeles) (c) Iterative Fair KD-tree (Los Angeles)

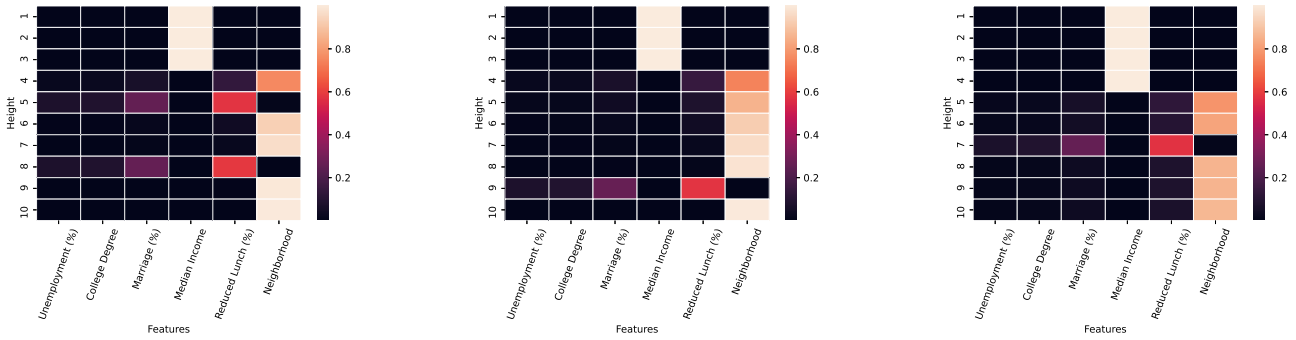

(d) Median KD-tree (Houston) (e) Fair KD-tree (Houston) (f) Iterative Fair KD-tree (Houston)

Figure 9: Impact of features on decision-making.

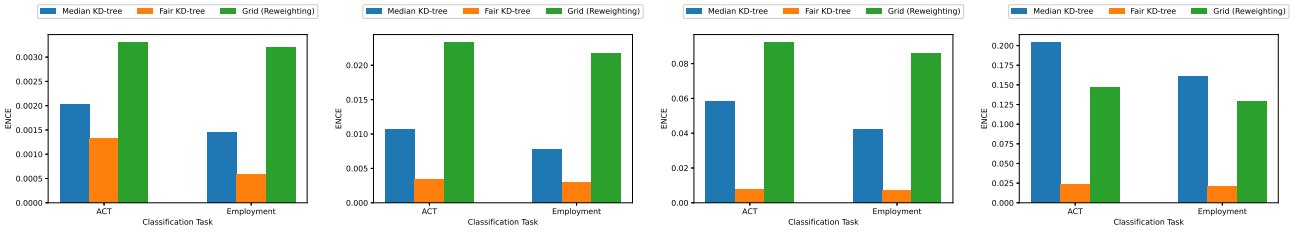

(a) Height= 4, Los Angeles (b) Height= 6, Los Angeles (c) Height= 8, Los Angeles (d) Height= 10, Los Angeles

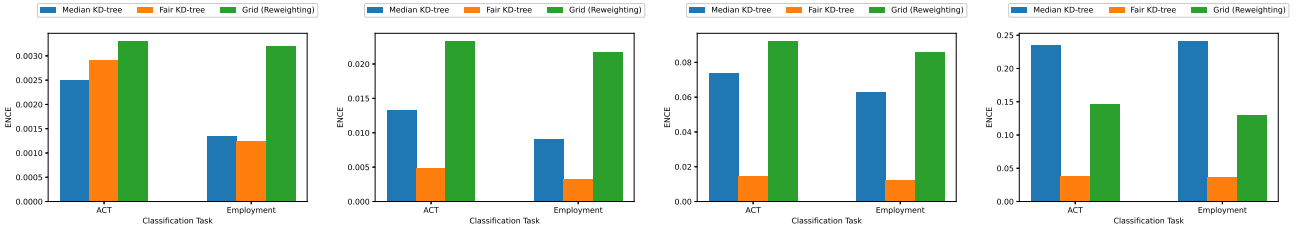

(e) Height= 4, Houston (f) Height= 6, Houston (g) Height= 8, Houston (h) Height= 10, Houston

Figure 10: Performance evaluation of multi-objective algorithm.

calibration of the model. As an example, consider the median KD-tree algorithm at the height of 8 in Los Angeles (Figure 8b): there is a sudden drop in training calibration, which can be explained by looking at the corresponding heat map in Figure 9a. At the height of 8, the influential features on decision-making consist of different elements than the heights 4, 6, and 10, leading to the fluctuation in the model calibration.

5.4 Performance of multi-objective approach.

When multi-objective criteria are used, we need a methodology to unify the geospatial boundaries generated by each task. Our proposed multi-objective fair partitioning predicated on Fair KD-trees addresses exactly this problem. In our experiments, we use the two criteria of ACT scores and employment percentage of families as the two objectives used for partitioning. These features

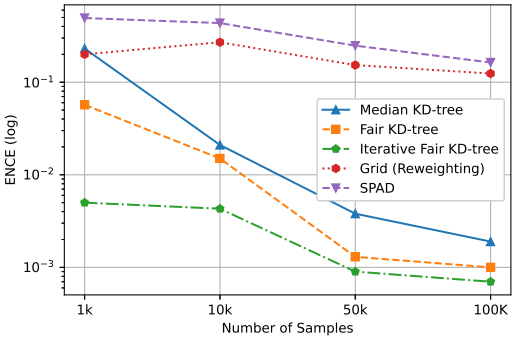

Figure 11: Performance evaluation on synthetic data.

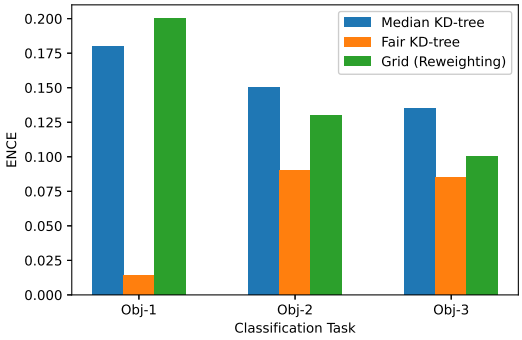

Figure 12: Multi-objective Performance Evaluation.

are separated from the training dataset in the pre-processing phase and are used to generate labels. The threshold for ACT is selected as before (22), and the threshold for label generation based on family employment is set to 10 percent.

Figure 10 presents the results of the Multi-Objective Fair KD-tree (to simplify chart notation, we use the 'Fair KD-tree' label). We choose a α value of 0.5 to give equal weight to both objectives. We emphasize that, the output of the Multi-Objective Fair KD-tree is a single non-overlapping partitioning of the space representing neighborhoods. Once the neighborhoods are generated, we show the performance with respect to each objective function, i.e., ACT and employment. The first row of the figure shows the performance for varying tree heights in Los Angeles, and the second row corresponds to Houston. The proposed algorithm improves fairness for both objective functions. The margin of improvement increases as the height of the tree increases.

5.5 Synthetic Data Results

We compare the studied algorithms using synthetic datasets, with the primary focus of assessing their performance on larger data cardinality. The results are illustrated in Figure 11. Synthetic data were generated with sizes of $1k$, $10k$, $50k$, $100k$ using Python's SKLearn library to create a classification task encompassing 5 features, and users were distributed across the Los Angeles map. The findings validate the earlier performance assessment using real-world data, highlighting the superior performance of both the Iterative Fair KD-tree and Fair KD-tree algorithms.

5.6 Multi-Objective Performance Evaluation

Figure 12 evaluates the Fair KD-tree's effectiveness in a multi-objective setting using synthetic data. We use three target features labeled as 'Obj1', 'Obj2', and 'Obj3'. The multi-objective fair KD-tree is used to generate a single unified map for all three, and the resulting performance is evaluated. The outcomes corroborate the performance analysis using real-world data, highlighting the improved fairness outcomes achieved by the Fair KD-tree algorithm.

6 CONCLUSION

We introduced an indexing method aimed at ensuring spatial group fairness in machine learning. This method divides the data domain, considering both geographical aspects and calibration errors. Comprehensive assessments on real-world data confirm our technique's efficacy in minimizing unfairness when training with location features, without compromising data utility. Looking ahead, we aim to delve deeper into custom split metrics for fairness-aware spatial indexing that acknowledges data distribution nuances. We will also explore other indexing frameworks, like R^+ trees, which fully encompass the data domain and offer enhanced clustering traits. Furthermore, our present framework is designed for binary classification. There's a need to adapt this model for multi-class classification.

Acknowledgments. This research has been funded in part by NIH grant R01LM014026, NSF grants IIS-1910950, IIS-1909806, CNS-2125530 and IIS-2128661, and an unrestricted cash gift from Microsoft Research. Any opinions, findings, conclusions or recommendations expressed in this material are those of the author(s) and do not necessarily reflect the views of any of the sponsors such as the NSF.

REFERENCES

[1] [n.d.]. National Center for Education Statistics. https://nces.ed.gov/
[2] 2015. Chicago Crime Dataset. https://data.cityofchicago.org/Public-Safety/Crimes-2015/vwwp-7yr9
[3] Nawal Benabbou, Mithun Chakraborty, and Yair Zick. 2019. Fairness and diversity in public resource allocation problems. *Bulletin of the Technical Committee on Data Engineering* (2019).
[4] Richard Berk, Hoda Heidari, Shahin Jabbari, Michael Kearns, and Aaron Roth. 2021. Fairness in criminal justice risk assessments: The state of the art. *Sociological Methods & Research* 50, 1 (2021), 3–44.
[5] Simon Caton and Christian Haas. 2020. Fairness in machine learning: A survey. *arXiv preprint arXiv:2010.04053* (2020).
[6] Alexandra Chouldechova. 2017. Fair prediction with disparate impact: A study of bias in recidivism prediction instruments. *Big data* 5, 2 (2017), 153–163.
[7] Cynthia Dwork, Moritz Hardt, Toniann Pitassi, Omer Reingold, and Richard Zemel. 2012. Fairness through awareness. In *Proceedings of the 3rd innovations in theoretical computer science conference*. 214–226.
[8] Cynthia Dwork and Christina Ilvento. 2018. Individual fairness under composition. *Proceedings of Fairness, Accountability, Transparency in Machine Learning* (2018).
[9] Ahmed Eldawy and Mohamed F Mokbel. 2015. Spatialhadoop: A mapreduce framework for spatial data. In *2015 IEEE 31st international conference on Data Engineering*. IEEE, 1352–1363.
[10] Evanthia Faliagka, Athanasios Tsakalidis, and Giannis Tzimas. 2012. An integrated e-recruitment system for automated personality mining and applicant ranking. *Internet research* (2012).
[11] Brian Fischer. 2021. data science methodology and applications. https://bookdown.org/bfischer_su/bookdown-demo/edgap.html
[12] Siamak Ghodsi, Harith Alani, and Eirini Ntoutsi. 2022. Context matters for fairness–a case study on the effect of spatial distribution shifts. *arXiv preprint arXiv:2206.11436* (2022).
[13] Chuan Guo, Geoff Pleiss, Yu Sun, and Kilian Q Weinberger. 2017. On calibration of modern neural networks. In *International conference on machine learning*. PMLR, 1321–1330.
[14] Moritz Hardt, Eric Price, and Nati Srebro. 2016. Equality of opportunity in supervised learning. *Advances in neural information processing systems* 29 (2016), 3315–3323.
[15] Alan M Hay. 1995. Concepts of equity, fairness and justice in geographical studies. *Transactions of the Institute of British Geographers* (1995), 500–508.
[16] Erhu He, Yiqun Xie, Xiaowei Jia, Weiye Chen, Han Bao, Xun Zhou, Zhe Jiang, Rahul Ghosh, and Praveen Ravirathinam. 2022. Sailing in the location-based fairness-bias sphere. In *Proceedings of the 30th International Conference on Advances in Geographic Information Systems*. 1–10.

[17] Matthew Joseph, Michael Kearns, Jamie H Morgenstern, and Aaron Roth. 2016. Fairness in learning: Classic and contextual bandits. *Advances in neural information processing systems* 29 (2016).

[18] Faisal Kamiran and Toon Calders. 2012. Data preprocessing techniques for classification without discrimination. *Knowledge and information systems* 33, 1 (2012), 1–33.

[19] Toshihiro Kamishima, Shotaro Akaho, Hideki Asoh, and Jun Sakuma. 2012. Fairness-aware classifier with prejudice remover regularizer. In *Joint European conference on machine learning and knowledge discovery in databases*. Springer, 35–50.

[20] Matthäus Kleindessner, Pranjal Awasthi, and Jamie Morgenstern. 2020. A Notion of Individual Fairness for Clustering. *arXiv preprint arXiv:2006.04960* (2020).

[21] Matt J Kusner, Joshua R Loftus, Chris Russell, and Ricardo Silva. 2017. Counterfactual fairness. *arXiv preprint arXiv:1703.06856* (2017).

[22] Michelle Seng Ah Lee and Luciano Floridi. 2021. Algorithmic fairness in mortgage lending: from absolute conditions to relational trade-offs. *Minds and Machines* 31, 1 (2021), 165–191.

[23] Sepideh Mahabadi and Ali Vakilian. 2020. Individual fairness for k-clustering. In *International Conference on Machine Learning*. PMLR, 6586–6596.

[24] Ninareh Mehrabi, Fred Morstatter, Nripsuta Saxena, Kristina Lerman, and Aram Galstyan. 2021. A survey on bias and fairness in machine learning. *ACM Computing Surveys (CSUR)* 54, 6 (2021), 1–35.

[25] Vishwali Mhasawade, Yuan Zhao, and Rumi Chunara. 2021. Machine learning and algorithmic fairness in public and population health. *Nature Machine Intelligence* 3, 8 (2021), 659–666.

[26] Mahdi Pakdaman Naeini, Gregory Cooper, and Milos Hauskrecht. 2015. Obtaining well calibrated probabilities using bayesian binning. In *Twenty-Ninth AAAI Conference on Artificial Intelligence*.

[27] Dana Pessach and Erez Shmueli. 2022. A review on fairness in machine learning. *ACM Computing Surveys (CSUR)* 55, 3 (2022), 1–44.

[28] John Platt et al. 1999. Probabilistic outputs for support vector machines and comparisons to regularized likelihood methods. *Advances in large margin classifiers* 10, 3 (1999), 61–74.

[29] Geoff Pleiss, Manish Raghavan, Felix Wu, Jon Kleinberg, and Kilian Q Weinberger. 2017. On fairness and calibration. *Advances in neural information processing systems* 30 (2017).

[30] David Pujol and Ashwin Machanavajjhala. 2021. Equity and Privacy: More Than Just a Tradeoff. *IEEE Security & Privacy* 19, 6 (2021), 93–97.

[31] Christopher Riederer and Augustin Chaintreau. 2017. The Price of Fairness in Location Based Advertising. (2017).

[32] Dimitris Sacharidis, Giorgos Giannopoulos, George Papastefanatos, and Kostas Stefanidis. 2023. Auditing for Spatial Fairness. *arXiv preprint arXiv:2302.12333* (2023).

[33] Sina Shaham, Gabriel Ghinita, and Cyrus Shahabi. 2022. Models and Mechanisms for Fairness in Location Data Processing. *arXiv preprint arXiv:2204.01880* (2022).

[34] Suraj Shetiya, Ian P Swift, Abolfazl Asudeh, and Gautam Das. 2022. Fairness-aware range queries for selecting unbiased data. In *2022 IEEE 38th International Conference on Data Engineering (ICDE)*. IEEE, 1423–1436.

[35] Peter VanWylen. [n.d.]. Visualizing the education gap. https://www.edgap.org/#6/37.886/-97.000

[36] Caroline Wang, Bin Han, Bhrij Patel, and Cynthia Rudin. 2022. In pursuit of interpretable, fair and accurate machine learning for criminal recidivism prediction. *Journal of Quantitative Criminology* (2022), 1–63.

[37] Yongzhi Wang, Hua Lv, and Yuqing Ma. 2020. Geological tetrahedral model-oriented hybrid spatial indexing structure based on Octree and 3D R*-tree. *Arabian Journal of Geosciences* 13 (2020), 1–11.

[38] Leonard Weydemann, Dimitris Sacharidis, and Hannes Werthner. 2019. Defining and measuring fairness in location recommendations. In *Proceedings of the 3rd ACM SIGSPATIAL international workshop on location-based recommendations, geosocial networks and geoadvertising*. 1–8.

[39] Yiqun Xie, Erhu He, Xiaowei Jia, Weiye Chen, Sergii Skakun, Han Bao, Zhe Jiang, Rahul Ghosh, and Praveen Ravirathinam. 2022. Fairness by "Where": A Statistically-Robust and Model-Agnostic Bi-level Learning Framework. In *Proceedings of the AAAI Conference on Artificial Intelligence*, Vol. 36. 12208–12216.

[40] Chengyuan Zhang, Ying Zhang, Wenjie Zhang, and Xuemin Lin. 2016. Inverted linear quadtree: Efficient top k spatial keyword search. *IEEE Transactions on Knowledge and Data Engineering* 28, 7 (2016), 1706–1721.

A APPENDIX

A.1 Expected Calibration Error

Expected Calibration Error (ECE) is one of the primary metrics used to quantify calibration in ML. According to this metric, the output confidence scores are sorted and partitioned into M bins denoted by B_1, ..., B_m. The associated score for each data instance lies within one of the bins. The ECE metric is then calculated over bins as follows:

$$\text{ECE} = \sum_{m=1}^{M} \frac{B_m}{n} |\text{o}(B_m) - e(B_m)| \tag{15}$$

A.2 Theorem Proofs

Proof of Theorem 1

The proof follows triangle inequality. The weighted calibration of the model can be written as,

$$\sum_{N_i \in \mathcal{N}} |N_i| \times |e(h|N = N_i) - o(h|N = N_i)| = \tag{16}$$

$$\sum_{N_i \in \mathcal{N}} |N_i| \times |\frac{1}{|N_i|}(\sum_{u \in N_i} s_u) - \frac{1}{|N_i|}(\sum_{u \in N_i} y_u)| = \tag{17}$$

$$\sum_{N_i \in \mathcal{N}} |\sum_{u \in N_i} s_u - \sum_{u \in N_i} y_u| \geq |\sum_{u \in D} s_u - \sum_{u \in D} y_u| \tag{18}$$

$$= |D| \times (|e(h) - o(h)|) \tag{19}$$

Proof of Theorem 2

Since $\mathcal{N}_2$ is a subgroup partitioning of $\mathcal{N}_1$ it can be constructed following step-by-step partitioning of neighborhoods in $\mathcal{N}_1$ into finer granularity ones until reaching $\mathcal{N}_2$. Denote $\mathcal{N}_1$ neighborhoods by $\{N_1, N_2, ..., N_t\}$. Without loss of generality, we show that splitting an arbitrary neighborhood $N_j \in \mathcal{N}_1$ to N_{j1} and N_{j2} leads to a worse ENCE metric value:

$$\text{ENCE}(\mathcal{N}_1) = \sum_{N_i \in \mathcal{N}} |N_i| \times |e(h|N = N_i) - o(h|N = N_i)| = \tag{20}$$

$$\sum_{N_i \in \mathcal{N}, i \neq j} |N_i| \times |e(h|N = N_i) - o(h|N = N_i)| +$$

$$|N_j| \times |e(h|N = N_j) - o(h|N = N_j)| \tag{21}$$

Note that,

$$|N_j| \times |e(h|N = N_j) - o(h|N = N_j)| = \tag{22}$$

$$|N_j| \times |\frac{1}{|N_j|}(\sum_{u \in N_j} s_u) - \frac{1}{|N_j|}(\sum_{u \in N_j} y_u)| = \tag{23}$$

$$|(\sum_{u \in N_j} s_u) - (\sum_{u \in N_j} y_u)| = \tag{24}$$

$$|(\sum_{u \in N_{j1}} s_u) - (\sum_{u \in N_{j1}} y_u) + (\sum_{u \in N_{j2}} s_u) - (\sum_{u \in N_{j2}} y_u)| \leq \tag{25}$$

$$|(\sum_{u \in N_{j1}} s_u) - (\sum_{u \in N_{j1}} y_u)| + |(\sum_{u \in N_{j2}} s_u) - (\sum_{u \in N_{j2}} y_u)| = \tag{26}$$

$$|N_{j1}| \times |\frac{1}{|N_{j1}|}(\sum_{u \in N_{j1}} s_u) - \frac{1}{|N_{j1}|}(\sum_{u \in N_{j1}} y_u)| +$$

$$|N_{j2}| \times |\frac{1}{|N_{j2}|}(\sum_{u \in N_{j2}} s_u) - \frac{1}{|N_{j2}|}(\sum_{u \in N_{j2}} y_u)| \tag{27}$$

Therefore, since by further splitting of neighborhoods, ENCE gets worse and as $\mathcal{N}_2$ can be reconstructed one division at a time from $\mathcal{N}_1$, one can conclude that

$$\text{ENCE}(N_1) \leq \text{ENCE}(N_2) \tag{28}$$

Proof of Theorem 3

As the tree is binary, there is a maximum of $\lceil \log(t) \rceil$ partitioning levels. At every level of the tree, the fairness objective function is calculated $|D|$ times, with each computation taking a constant time. Therefore, the required number of computations is

$O(|D| \times \lceil \log(t) \rceil)$. Moreover, the algorithm requires an initial run of the model h, which depends on what ML model is employed, represented by the computation complexity of $O(h)$ in the total complexity equation.

Proof of Theorem 4

Similar to Fair KD-tree, the total number of levels in Iterative Fair KD-tree is $\lceil \log(t) \rceil$ requiring computational complexity of $O(|D| \times \lceil \log(t) \rceil)$ to obtain the values for fair partitioning. However, in contrast to the Fair KD-tree algorithm, the iterative version requires the execution of the ML model at every height of the tree. The total computational complexity adds up to $O(|D| \times \lceil \log(t) \rceil) + \lceil \log(t) \rceil \times O(h)$.

Proof of Theorem 5

Multi-objective Fair KD-tree requires a single execution of the ML classifier at the beginning of the algorithm. Therefore, the computational complexity is $\sum_{i=1}^{m} O(h_i)$. Once confidence scores are generated, given that m is small, the total required objective computations at every tree level remains $O(|D| \times \lceil \log(t) \rceil)$ as the combined vector can be calculated in constant time.